Journal of Organometallic Chemistry 695 (2010) 1215–1224

Contents lists available at ScienceDirect

Journal of Organometallic Chemistry

journal homepage: www.elsevier.com/locate/jorganchem

# New morpholine- and piperazine-functionalized triphenylantimony(V) catecholates: The spectroscopic and electrochemical studies

Andrey I. Poddel'sky [a,*], Ivan V. Smolyaninov [b], Yury A. Kurskii [a], Georgy K. Fukin [a], Nadezhda T. Berberova [b], Vladimir K. Cherkasov [a], Gleb A. Abakumov [a]

[a] G.A. Razuvaev Institute of Organometallic Chemistry, Russian Academy of Sciences, 49 Tropinina Street, 603950 Nizhny Novgorod, Russia
[b] Southern Scientific Center, Russian Academy of Sciences, 41 Chekhova Street, 344006 Rostov-on-Don, Russia

ARTICLE INFO

*Article history:*
Received 17 September 2009
Received in revised form 13 January 2010
Accepted 24 January 2010
Available online 1 February 2010

*Keywords:*
Antimony
Catecholates
Dioxygen
X-ray diffraction
NMR spectroscopy
Cyclic voltammometry

ABSTRACT

Novel functionalized triphenylantimony(V) catecholates – $Ph_3Sb[4\text{-}O(CH_2CH_2)_2N\text{-}3,6\text{-}DBCat]$ (**1**), $Ph_3Sb[4\text{-}PhN(CH_2CH_2)_2N\text{-}3,6\text{-}DBCat]$ (**2**), $Ph_3Sb[4\text{-}Ph_2CHN(CH_2CH_2)_2N\text{-}3,6\text{-}DBCat]$ (**3**), $Ph_3Sb[4,5\text{-}Piperaz\text{-}3,6\text{-}DBCat]$ (**4**) and binuclear bis-catecholate $Ph_3Sb[3,6\text{-}DBCat\text{-}4\text{-}N(CH_2CH_2)_2N\text{-}4\text{-}3,6\text{-}DBCat]SbPh_3$ (**5**) were synthesized by the oxidative addition reaction of corresponding *o*-quinones with triphenylantimony. The $[4\text{-}O(CH_2CH_2)_2N\text{-}3,6\text{-}DBCat]^{2-}$, $[4\text{-}PhN(CH_2CH_2)_2N\text{-}3,6\text{-}DBCat]^{2-}$, $[4\text{-}Ph_2CHN(CH_2CH_2)_2N\text{-}3,6\text{-}DBCat]^{2-}$ and $[4,5\text{-}Piperaz\text{-}3,6\text{-}DBCat]^{2-}$ are 4-(morpholin-1-yl)-, 4-(4-phenyl-piperazin-1-yl)-, 4-(4-dephenylmethyl-piperazin-1-yl)-, and 4,5-(piperazin-1,4-diyl)-3,6-di-*tert*-butyl-catecholate dianionic ligands, correspondingly. Complexes **1–5** were characterized in details by IR-, $^1H$ and $^{13}C$ NMR spectroscopy and cyclic voltammometry. Molecular structure of $\mathbf{4}\cdot CH_3OH$ was determined by X-ray crystallography to be a distorted tetragonal–pyramidal. The NMR spectroscopic and electrochemical investigations of complexes in the presence of air reveal the reactions of complexes with dioxygen leading to the formation of spiroendoperoxides of 1,2,4,3-trioxastibolane type in a NMR yield of 25–37%.



## 1. Introduction

At the present time the coordination chemistry of antimony is the one of the fast developing branches of organoelemental chemistry. Organoantimony complexes attract attention of researchers because of their activity in a number of reactions in organic synthesis [1], the application in medicine and pharmacy, etc. [2]. On the other hand, metal complexes with redox-active *o*-benzoquinonato type ligands reveal a diversity of interesting and sometimes intriguing properties such as intramolecular electron transfer "metal–ligand" induced by coordination sphere transformations [3], phenomenon of redox-isomerism and photo/thermomechanical effect [4], "wandering" valence – the characteristic feature of mixed-ligand *o*-semiquinone/catecholate non-transition metal complexes [5], and more. These features are caused by the redox-active nature of ligands based on *o*-benzoquinones. In complexes, *o*-semiquinolate and catecholate forms are stable and able to turn one to another by one-electron reduction and oxidation.

Recently, we have found one more unique property of antimony complexes with redox-active ligands: *o*-amidophenolato triphenylantimony(V) complexes are the first non-transition element compounds which can reversibly bind molecular oxygen [6]. This unique property is rationalized by the easy one-electron oxidation of *o*-amidophenolato dianion to *o*-iminobenzosemiquinonato radical-anion in the antimony(V) coordination sphere by molecular oxygen. This process was supposed to be a key stage in mechanism of reversible $O_2$ binding [6]. The search of other compounds with this peculiar properties have resulted in the synthesis of $O_2$-active catecholate triphenylantimony(V) complexes with electron-donor groups in Cat ligand [7]. Contrariwise, electron-withdrawing substituents of Cat ligand make the complex derived to be air-stable [8].

In this paper we report on the synthesis and characterization of new triphenylantimony(V) catecholates with weak electron-donor nitrogen-containing substituents in 4- (4,5-) position of 3,6-di-*tert*-butyl-catecholate.

## 2. Results and discussion

### 2.1. Syntheses and characterizations

Previously, different ways to Sb(V) catecholate complexes have been reported [8,9]. There is a reaction of triphenylantimony dichloride and catechol in the presence of ammonia [9a], an oxidation of

* Corresponding author. Address: G.A. Razuvaev Institute of Organometallic Chemistry, Russian Academy of Sciences, 49 Tropinina Street, GSP-445, 603950 Nizhny Novgorod, Russia. Fax: +7 831 462 74 97.
*E-mail address:* aip@iomc.ras.ru (A.I. Poddel'sky).

0022-328X/$ - see front matter © 2010 Elsevier B.V. All rights reserved.
doi:10.1016/j.jorganchem.2010.01.029

elemental antimony by the *o*-quinones [9b], the oxidation of $R_3Sb$ (R = Ph, Me) with *tert*-butylhydroperoxide in the presence of catechol and neutral donor ligands L [9c], and finally an oxidative addition reaction between antimony(III) compounds by *o*-quinones [8,9d,9e]. In our case, the later way was chosen as the most suitable method to prepare triphenylantimony(V) catecholates (Schemes 1 and 2). The corresponding neutral *o*-benzoquinones **$Q^1$–$Q^4$** were synthesized as reported in Ref. [10].

The slow addition of 2 equiv. of $SbPh_3$ to the toluene solution of bis-*o*-quinone with piperazine bridge allows to prepare binuclear triphenylantimony(V) bis-catecholate **5**.

In all cases after a number of steps (see Section 4), the slow evaporation of the hexane solution of the complexes **1**–**4** afforded microcrystalline pale-yellow or yellow material that was identified by IR-, $^1H$, $^{13}C$ and DEPT NMR spectroscopy and elemental analysis. Molecular structure of **4** was determined by X-ray crystallography.

### 2.2. IR spectroscopy

The formation of catecholate complexes is evident from a number of typical bands of their IR spectra in the range of 700–1600 $cm^{-1}$ [11a,b]. The absence of stretching vibrations of double C=O bonds at 1650–1750 $cm^{-1}$ verifies the absence of initial unreduced *o*-quinones in complexes samples. The stretching vibrations of catecholate single C–O bonds in **1**–**5** give rise to a number of bands in the region 1170–1300 $cm^{-1}$. IR spectra of complexes contain a set of bands typical for functional substituents at Cat ligand (the oxygen–carbon–oxygen asymm. and symm. vibrations of morpholine fragment in **1**, $\nu$(O–C–O) 1095 and 920 $cm^{-1}$; the carbon–nitrogen vibrations of morpholine and piperazine groups in **1**–**5** – a set of bands at 930–1150 and 770–850 $cm^{-1}$) as well as $O_2SbPh_3$ moiety (skeleton vibrations of $SbPh_3$ are observed at ~690 and ~730 $cm^{-1}$ for all complexes, stretching vibrations Sb–O are at 620–650 $cm^{-1}$, while stretching vibrations Sb–$C_{Ph}$ lie in the region 440–470 $cm^{-1}$) [11c].

### 2.3. Crystal structure of *4*

The crystal structure catecholate **4** was determined by single-crystal X-ray diffraction analysis. The X-ray quality crystals were grown by the recrystallization of **4** from methanol as the methanol solvate **4**·$CH_3OH$. Molecular structure complex **4**·$CH_3OH$ is depicted in Fig. 1; the selected bond lengths and angles are listed in Table 1; Table 2 shows the experimental and refinement details of X-ray study.

The coordination environment of antimony atom has a distorted octahedral geometry where the axial atoms are C(15) of phenyl group and O(1S) of donor molecule (methanol). The angle O(1S)–Sb(1)–C(15) of 173.60(4)° is the most right angle among bond angles of central antimony atom. The catecholate ligand and two phenyl groups lie in equatorial plane; the sum of angles near antimony atom at O(1)O(2)C(21)C(27) plane is 354.01(4)°. The deviation of Sb(1) from this plane toward the axial phenyl group is 0.336(1) Å. The angles between equatorial groups and axial Ph substituent are in the range of 96.53–101.40(4)°. The five-membered metallocycle in **4**·$CH_3OH$ is not planar like other

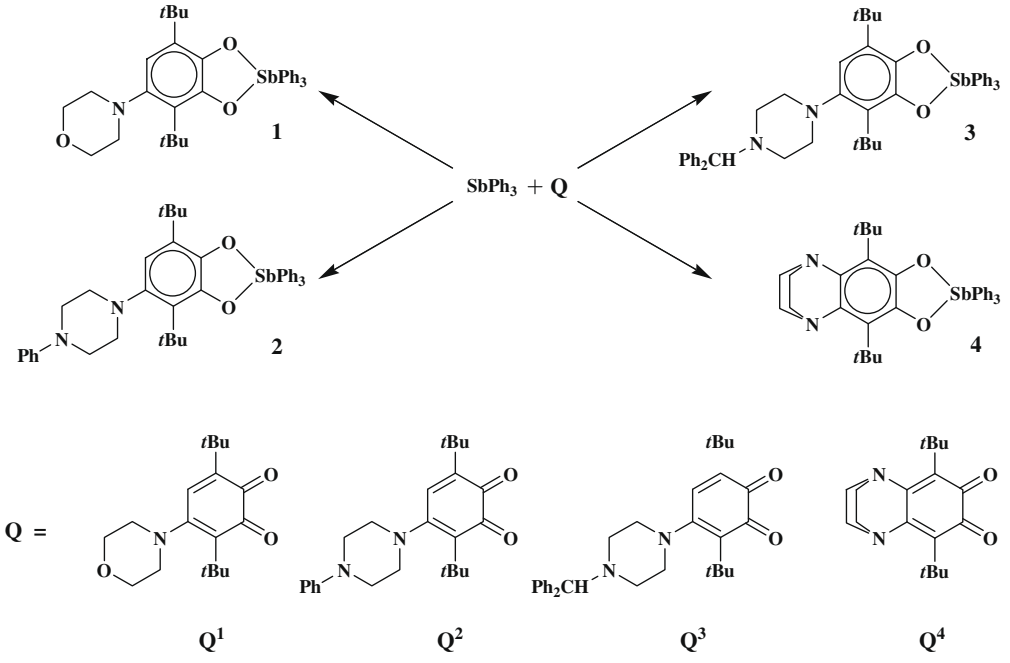


**Scheme 1.**


$Ph_3Sb$[3,6-DBCat]-Piperaz-[3,6-DBCat]$SbPh_3$ **5**

**Scheme 2.**

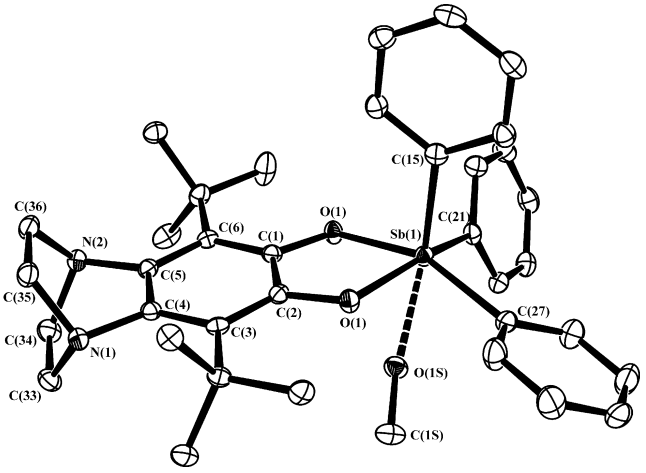


**Fig. 1.** An ORTEP view of **4**·$CH_3OH$ (H atoms are omitted for clarity).

**Table 1**
The selected bond lengths and angles in **4**·$CH_3OH$.

| Distance (Å) | | Angle (°) | |
|---|---|---|---|
| Sb–O(1) | 2.0198(9) | O(1)–Sb(1)–O(2) | 78.58(3) |
| Sb–O(2) | 2.0308(8) | O(1)–Sb(1)–C(15) | 96.53(4) |
| Sb–C(15) | 2.1227(11) | O(2)–Sb(1)–C(15) | 96.99(4) |
| Sb–C(27) | 2.1481(13) | O(1)–Sb(1)–C(27) | 158.61(4) |
| Sb–C(21) | 2.1487(11) | O(2)–Sb(1)–C(27) | 87.70(4) |
| Sb–O(S) | 2.5071(8) | C(15)–Sb(1)–C(27) | 101.40(5) |
| O(1)–C(1) | 1.3658(13) | O(1)–Sb(1)–C(21) | 86.37(4) |
| O(2)–C(2) | 1.3595(15) | O(2)–Sb(1)–C(21) | 157.64(4) |
| N(1)–C(4) | 1.4601(14) | C(15)–Sb(1)–C(21) | 101.10(4) |
| N(2)–C(5) | 1.4616(16) | C(27)–Sb(1)–C(21) | 101.36(5) |
| C(1)–C(6) | 1.4005(18) | O(1)–Sb(1)–O(1S) | 78.17(3) |
| C(1)–C(2) | 1.4238(16) | O(2)–Sb(1)–O(1S) | 78.53(3) |
| C(2)–C(3) | 1.4039(15) | C(15)–Sb(1)–O(1S) | 173.60(4) |
| C(3)–C(4) | 1.4084(18) | C(27)–Sb(1)–O(1S) | 83.10(4) |
| C(3)–C(7) | 1.5508(15) | C(21)–Sb(1)–O(1S) | 82.29(4) |
| C(4)–C(5) | 1.3945(16) | C(1)–O(1)–Sb(1) | 116.10(7) |
| C(5)–C(6) | 1.4108(15) | C(2)–O(2)–Sb(1) | 115.77(7) |

antimony(V) catecholates [7b,8a,9c], however, the bending angle along O(1)···O(2) line is 0.9(3)° that is the lowest among similar complexes. The Sb(1)–O(1) and Sb(1)–O(2) bonds differ slightly (2.0198(9) and 2.0308(8) Å, respectively); Sb–$C_{Ph}$ distances reveal different trans-effect of O,O-chelating catecholate ligand and donor methanol molecule: Sb(1)–C(21) and Sb(1)–C(27) *trans*-positioned toward catecholate oxygens are of 0.025 Å longer than the Sb(1)–C(15) distance (Table 1).

The geometrical characteristics of O,O′-chelating ligand (see Table 1) are in the consistence with dianionic coordination type (catecholate): for example, oxygen-to-carbon distances O(1)–C(1) of 1.3658(13) Å and O(2)–C(2) of 1.3595(15) Å are usual for antimony(V) catecholates (1.35–1.38 Å) [7–9]; and carbon-to-carbon bonds of the hexa-membered carbon ring are 1.409 ± 0.014 Å reflecting its aromatic character. The piperazine nitrogens N(1) and N(2) lie in the catecholate plane. Noteworthy is that *tert*-butyls are rotated around C–C bond with catecholate carbon cycle in a such manner where two methyls of *t*Bu are directed outside of central atom and third methyl is to oxygen-oriented while in the case of other most complexes of related O,O- and O,N-ligands this situation is inverted [7–9,12].

### 2.4. NMR spectroscopy

#### 2.4.1. Air-free conditions

$^1$H NMR spectra of mononuclear catecholates **1**–**3** have common features such as two singlets from two groups of *tert*-butyl protons (at 1.41–1.42 and 1.56–1.61 ppm), one singlet due to one isolated aromatic proton of Cat ligand (6.63–6.70 ppm); two multiplets from $SbPh_3$ moieties (in region of 7.40–7.83 ppm). At the same time, NMR spectra reveal differences reflecting the N-substituent presence in complexes: morpholine group in **1** gives rise to multiplets at 2.64–2.70 and 2.93–3.06 ppm from (–$CH_2$)$_2$N– fragment protons, and multiplet at 3.66–3.90 ppm from four protons of (–$CH_2$)$_2$O fragment; two multiplets at 2.91–3.11 and 3.51–3.59 ppm are due to piperazine protons in **2** while the sane protons in **3** have more complicated signal in NMR spectrum appearing as three multiplets at 2.17–2.21, 2.69–2.85 and 2.90–3.08 ppm.

The symmetric structure of bicyclic catecholate **4** is justified by its $^1$H NMR spectrum (Fig. 2, top) showing singlet from 2 equiv. *tert*-butyl groups (1.60 ppm), and two symmetrical multiplets at 2.54–2.75 and 2.86–3.07 ppm (with centers at $\delta$ = 2.63 and 2.98 ppm, correspondingly) due to eight protons of –N(–$CH_2$–$CH_2$–)$_2$N– moiety. These protons form spin system AA′BB′.

According to $^1$H NMR data (Fig. 2, bottom), binuclear complex **5** also has a symmetrical structure where two (Cat)$SbPh_3$ fragments are equal. Bridge piperazine protons appear as two multiplets (at 2.73–2.76 and 3.03–3.07 ppm with centers at $\delta$ = 2.75 and $\delta$ = 3.05 ppm) of the same form as those in NMR of **4**. Both the isolated aromatic protons of Cat ligands appear as singlet at 6.72 ppm, while *tert*-butyls give rise to two intense singlets (1.44 and 1.66 ppm) each from 18 protons of two *t*Bu groups. So, NMR spectroscopic data reveal that binuclear complex **5** has a symmetrical geometry containing piperazine bridge being in a chair conformation only because a bath conformation of the latter should lead to non-equivalence of (Cat)$SbPh_3$ moieties in NMR.

**Table 2**
Summary of crystal and refinement data for complex **4**·$CH_3OH$.

| | |
|---|---|
| Empirical formula | $C_{37}H_{45}N_2O_3Sb$ |
| Formula weight | 687.50 |
| $T$ (K) | 100(2) |
| Wavelength (Å) | 0.71073 |
| Crystal system | Triclinic |
| Space group | $P\bar{1}$ |
| *Unit cell dimensions* | |
| $a$ (Å) | 10.0526(2) |
| $b$ (Å) | 11.8361(3) |
| $c$ (Å) | 14.5638(3) |
| $\alpha$ (°) | 88.56 |
| $\beta$ (°) | 82.17° |
| $\gamma$ (°) | 68.61 |
| Volume (Å$^3$) | 1597.91(6) |
| $Z$ | 2 |
| $D_{calc}$ (Mg/m$^3$) | 1.429 |
| Absorption coefficient (mm$^{-1}$) | 0.902 |
| Crystal size (mm$^3$) | 0.31 × 0.28 × 0.21 |
| Theta range for data collection | 1.85–26.00 |
| Reflections collected | 9703 |
| Independent reflections [$R_{int}$] | 6252 [0.0103] |
| Absorption correction | Semi-empirical from equivalents |
| Max. and min. transmission | 0.8331 and 0.7673 |
| Refinement method | Full-matrix least-squares on $F^2$ |
| Data/restraints/parameters | 6252/3/568 |
| Final $R$ indices [$I > 2\sigma(I)$] | $R_1$ = 0.0197, $wR_2$ = 0.0491 |
| $R$ indices (all data) | $R_1$ = 0.0209, $wR_2$ = 0.0497 |
| Goodness-of-fit on $F^2$ | 1.001 |
| Largest diff. peak and hole (e Å$^{-3}$) | 0.811 and −0.281 |

#### 2.4.2. Air exposure conditions

One of, may be, the most unexpected chemical properties of triphenylantimony(V) catecholates and *o*-amidophenolates is the molecular oxygen binding with a reversible character [6]. As mentioned above, the insertion of strong donor substituents (one, two methoxy groups) in catecholate ligand of $CatSbPh_3$ complex

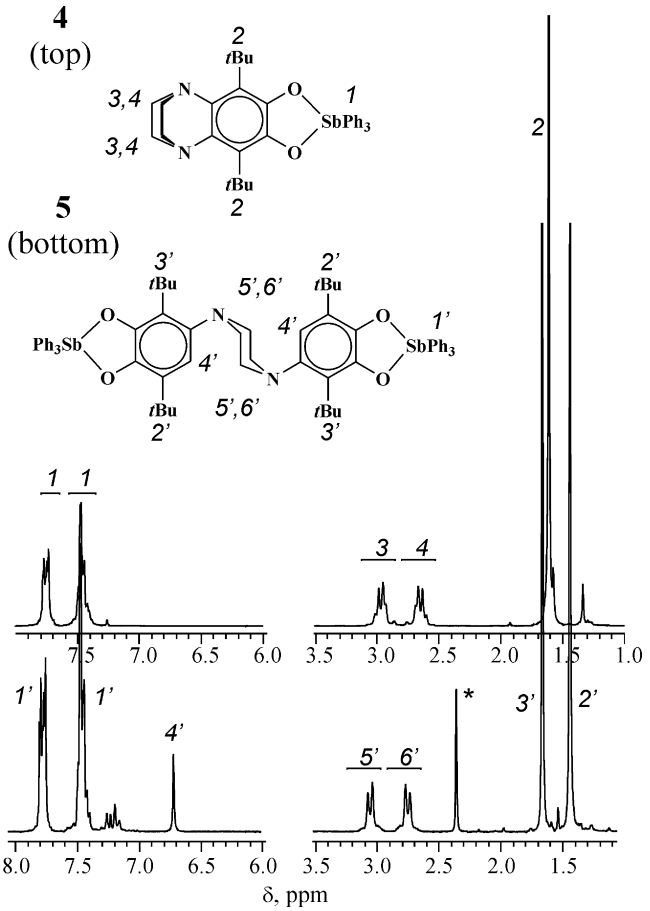


**Fig. 2.** $^1$H NMR spectra of mononuclear catecholate **4** (top) and binuclear catecholate **5** (bottom) in $CDCl_3$, RT. * peak is due to solvent toluene $CH_3$ group.

increases its reactivity toward dioxygen [7] contrary to different acceptor groups which inactivate the corresponding antimony catecholate complex in the reaction with molecular oxygen [8]. In the present case, Cat ligand in **1**–**4**, **5** contains weak donor group (morpholine, substituted piperazine). What will be the behaviour of these complexes in the presence of air?

The solutions of complexes **1**–**4** in $CDCl_3$ were exposed to air and $^1$H NMR monitoring gave the following results: in fact, all complexes react with molecular oxygen (Scheme 3). However, as it was expected, the conversion of this interaction is remarkably less than that one in the case of catecholates with strong electron-donor

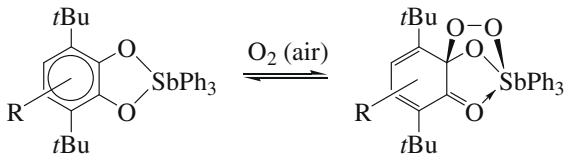


| $Ph_3Sb$(4-R-3,6-Cat) | $Ph_3Sb$[(R)L'$O_2$] | Yield |
|---|---|---|
| **1** (R = Morph) | **1a** | 33% |
| **2** (R = Ph-pyperaz) | **2a** | 25% |
| **3** (R = $Ph_2CH$-pyperaz) | **3a** | 30% |
| **4** | **4a** | 37% |

**Scheme 3.**

methoxy groups [7]. The conversion to dioxygen-bound complexes **1a**–**4a** is 25–37% (Scheme 3) compared with >90% for (4,5-dimethoxy-3,6-di-*tert*-butyl-catecholato)triphenylantimony(V) [7].

So, catecholates **1**–**4** are less inclined to form spiroendoperoxides on air than their methoxy-substituted analogues and the equilibrium between **1**–**4** and **1a**–**4a** is established sooner. The performed electrochemical data confirm NMR results (see below).

Fig. 3 shows the changes in $^1$H NMR spectra of complexes **2** and **4** in the presence of air. The $^1$H NMR spectrum of **2** on air reveal the appearance of signals from two pairs of *tert*-butyl groups (the first pair gives singlets at $\delta$ = 1.24 and 1.37 ppm and the second pair – at $\delta$ = 1.28 and 1.32 ppm) and unresolved multiplets from piperazine fragment (they appear at 3.1–3.3 and 3.6–3.8 ppm) pertaining to spiroendoperoxide **2a**. The singlet from proton in fifth position of Cat carbon ring shifts from 6.70 ppm (for **2**) to 6.61 ppm (**2a**). Also, in $^1$H NMR spectrum of **2** on air, the multiplets from phenyl groups appear at 7.32–7.42, 7.50–7.60, 7.68–7.76 and 8.24–8.32 ppm. The degassing of NMR tube leads to restoring of $^1$H NMR spectrum of initial **2**. The observance of two pairs of *tert*-butyl groups for **2a** can testify to the formation of two isomers for oxygen-containing spiroendoperoxide **2a** with the relative ratio 1.0:0.4, approximately (Scheme 4). In this case, isomer **A** with peroxo-fragment *para*-positioned toward substituent in fourth position of Cat ligand (Scheme 4, left) prevails over *meta*-isomer **B** (Scheme 4, right). For related triphenylantimony(V) *o*-amidophenolates and catecholates with strong donor methoxy groups, their spiroendoperoxides contain *para*-isomers only [6,7].

Complexes **1** and **3** on air demonstrate the same behaviour. So, we can propose that these complexes form isomers with different position of peroxo-fragment and donor substituent unlike *o*-amidophenolates [6] or catecholates with strong donor metoxy-groups [7]. The proposed isomers for complex **4** are the enantiomers and should have identical NMR spectra that is observed in practice (Fig. 3).

Noteworthy, according to Scheme 4 for bis-catecholate **5** we should provide the formation of big number of isomers on air, and the most expected are *mono*-spiroendoperoxides $Ph_3Sb$[3,6-DBCat]-piperazine-**A** and $Ph_3Sb$[3,6-DBCat]-piperazine-**B**, and di-spiroendoperoxides **A**-piperazine-**A** and **A**-piperazine-**B**. The $^1$H NMR spectroscopy (Supplementary Fig. S1) supports this supposition.

### 2.5. Electrochemistry

The electrochemical properties of transition metal catecholate complexes are well known and extensively discussed [13], at the same time any information about the redox-transformation of dioxolene ligand in the antimony(III/V) catecholate derivatives is practically absent. The redox properties of complexes **1**–**4** were explored by the cyclic voltammetry in $CH_2Cl_2$ solutions at a glassy carbon and platinum working electrodes. The redox potentials of the complexes do not depend practically on the electrode material. The results of electrochemical investigations are summarized in Table 3. Redox potentials are referenced vs. $Fc^+$/Fc couple.

#### 2.5.1. Air-free conditions

The target complexes reveal variable electrochemical behaviour. Usually, the catecholate ligand is characterized by two redox transitions: catecholate – *o*-semiquinonate, *o*-semiquinonate – *o*-quinone. The 3,6-di-*tert*-butyl-calecholate complex $Ph_3Sb$(3,6-DBCat) is listed in Table 3 to provide such recognized picture, where the second stage is not fully reversible because of the weak coordination ability of *o*-quinone to central antimony(V) atom (Scheme 5).

The introduction of nitrogen atom in the fourth position of aromatic ring complicates an interpretation of redox features of

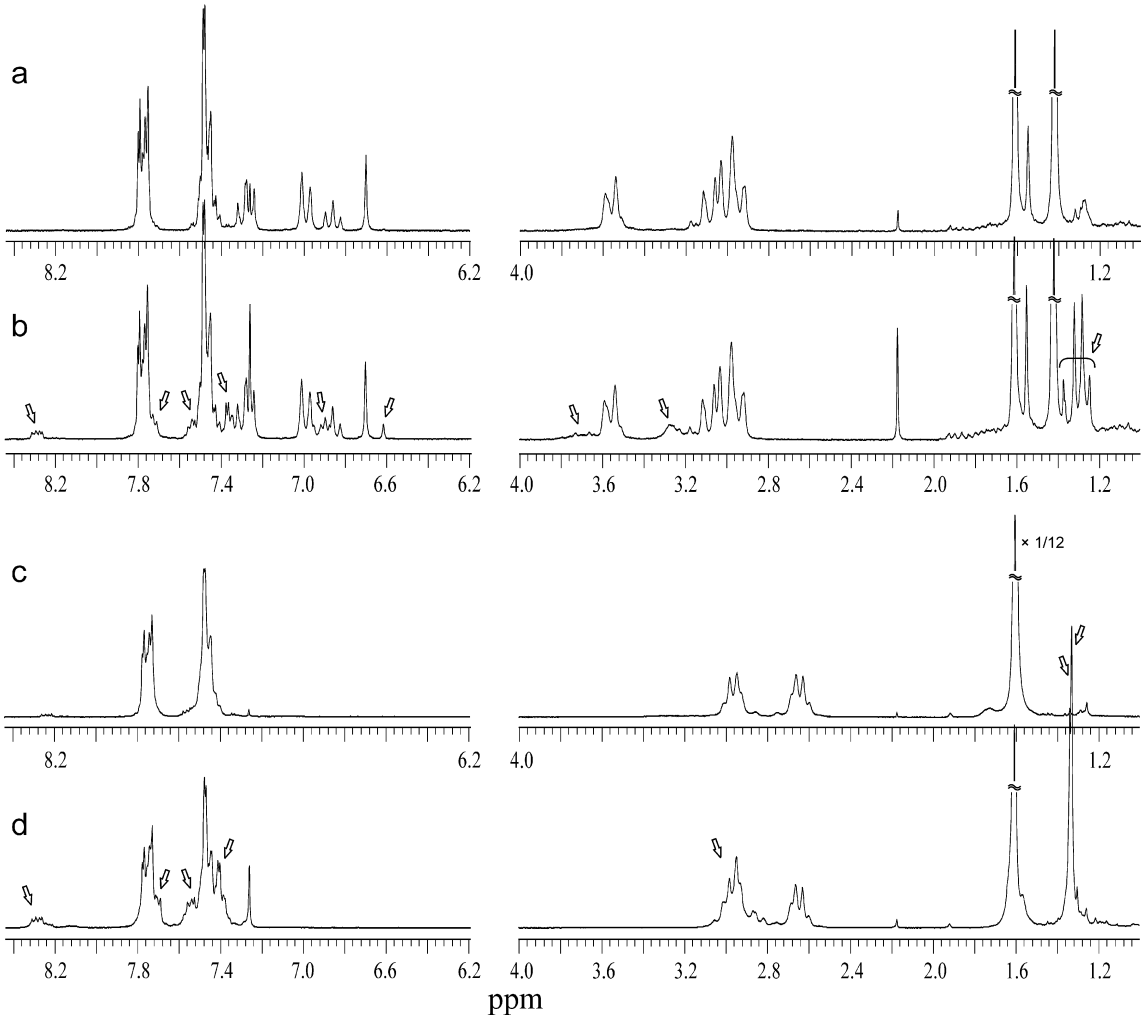


**Fig. 3.** The $^1$H NMR spectra of complexes **2** and **4** in vacuum (a and c) and in the presence of air (b and d) ($CDCl_3$, 298 K, standard TMS). Arrows show spectral lines from spiroendoperoxides.

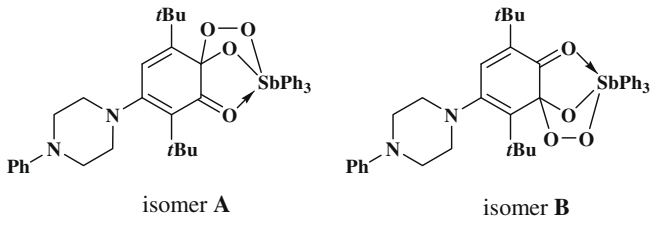


**Scheme 4.**

complexes **1**–**4** as the consequence of the two main reasons: (1) the redox activity of both the morpholine (piperazine) substituents and catecholate part and (2) the possibility of electronic interaction between two redox fragments owing to spin and charge localization in the semiquinone radical anion in fourth position of the ring. Supplementary Figs. S2–S5 of Supporting Information present the cyclic voltammograms of complexes. The first oxidation process for complexes has one electron irreversible nature, whereas the catechol – semiquinone oxidation is reversible process usually [13]. The insertion of donor nitrogen component leads to the potential drift (0.12–0.27 V) toward negative direction in comparison with $Ph_3Sb$(3,6-DBCat) complex, and the oxidation process is facilitated. The potential range of the first electrochemical stage is close to those for the aliphatic amines [14], however the antimony(V) catecholate complexes with donor substituents, for example ($Ph_3Sb$(4-MeO-3,6-DBCat), see Table 3), have the electrochemical activity at the same region. It is necessary to discuss redox transformations of each complex in detail. The influence of more electronegative oxygen atom is observed for complex **1** for the first electrochemical step. The difference between redox potentials ($E^1_p$) of complexes **1** and **2** is 0.07 V. This value is in agreement with the difference of the oxidation potential of morpholine, which is 0.80 V [15] and the piperazine fragment 0.75 V [16]. In the range of switching potentials ((−0.4)/(+0.6) V) on the CV back scan of compounds **1**, **2** the products of chemical stage (−0.23 V) occurring after electrochemical oxidation are fixed. The morpholine and piperazine cycles can undergo breaking C–N bond and consequently the ring opening during oxidation as different aliphatic amines [17].

The complex **3** (where diphenylmethyl substituent is in the fourth position of piperazine cycle) has the three well distinctive oxidation waves (Fig. 4). The products of the chemical stage on the reverse scan are also fixed after several scans at different potentials (−0.37 V; −1.09 V).

The partly disjunction of two redox centers is provided by the spatial separation of catecholate (II on Scheme 6) and piperazine part (I on Scheme 6), and availability of the broad electron system at the fourth position of nitrogen in piperazine cycle. The oxidation

**Table 3**
Redox potentials (in Volts) of complexes from cyclic voltammetry.

| Compound | $E^1_p$ (V) | $n$ | $E^2_p$ (V) | $E^3_{1/2}$ (V) | $i_{pc}/i_{pa}$ | $n$ |
|---|---|---|---|---|---|---|
| $Ph_3Sb[4\text{-}O(CH_2CH_2)_2N\text{-}3,6\text{-}DBCat]$ (**1**) | 0.34 | 1.0 | – | 0.76 | 0.70 | $n < 1$ |
| $Ph_3Sb[4\text{-}PhN(CH_2CH_2)_2N\text{-}3,6\text{-}DBCat]$ (**2**) | 0.28 | $n < 1$ | 0.40 | 0.73 | 0.30 | 1.0 |
| $Ph_3Sb[4\text{-}Ph_2CHN(CH_2CH_2)_2N\text{-}3,6\text{-}DBCat]$ (**3**) | 0.20 | $n < 1$ | 0.36[a] | 0.94 | 0.58 | 1.0 |
| $Ph_3Sb[4,5\text{-}Piperaz\text{-}3,6\text{-}DBCat]$ (**4**) | 0.32 | 1.0 | – | 0.73 | 0.67 | 1.0 |
| $Ph_3Sb(4\text{-}MeO\text{-}3,6\text{-}DBCat)$ | 0.34[a] | 1.0 | – | 0.72[b] | – | $n < 1$ |
| $Ph_3Sb(3,6\text{-}DBCat)$ | 0.47[a] | 1.0 | – | 0.98[b] | – | $n < 1$ |

Conditions: $CH_2Cl_2$ solution containing 0.10 M $[N(n\text{-}Bu)_4]ClO_4$ supporting electrolyte, glassy carbon working electrode; scan rate 200 $mVs^{-1}$; ferrocene internal standard; ~3 mM [complex].
Peak potentials $E^1_p$ and $E^2_p$ are given for irreversible processes.
$i_{pc}/i_{pa}$ – current ratios. $n$ – number of electrons transferred during redox-process vs. ferrocene.
[a] $E_{1/2}$, quasi-reversible process.
[b] $E_p$, irreversible process.

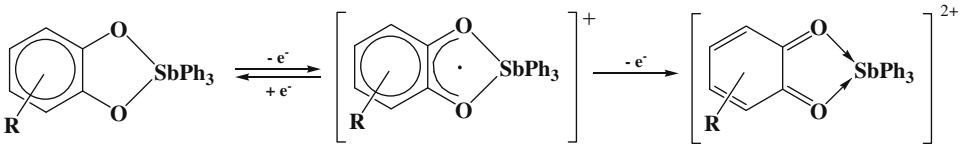


**Scheme 5.**

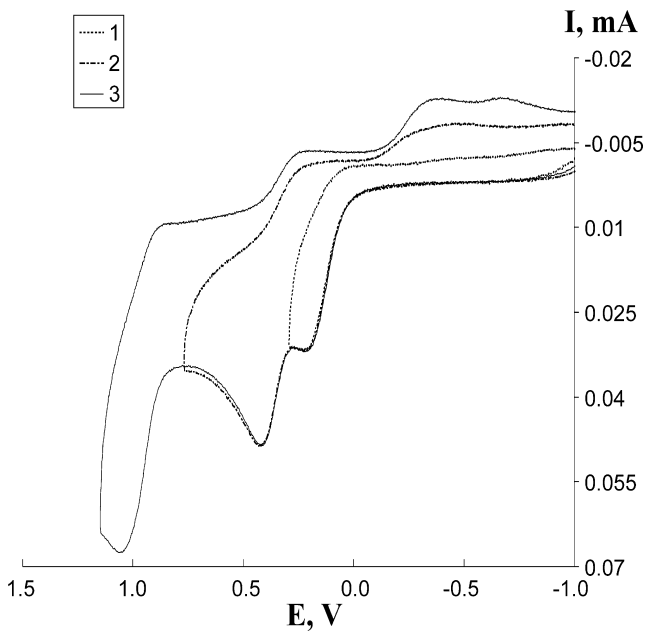


**Fig. 4.** Cyclic voltammogram of complex **3** ($3\cdot\times10^{-3}$ M) (switching potential 0.30 V (1); 0.80 V (2); 1.20 V (3)) in $CH_2Cl_2$ solution (0.10 M $Bu_4NClO_4$), glassy carbon working electrode at scan rates of 200 mV $s^{-1}$. Potentials are referenced in volts vs. $Fc^+/Fc$.

of nitrogen atom leads to unstable radical cation which can abstract proton from $CHPh_2$, which is observed at Pt-electrode (−0.43 V). This stage may lead to form diphenylmethyl radical or cycle opening (Scheme 6). The second reduction wave (−1.09 V) on the reverse scan is fixed in the range inherent to *o*-quinone's reduction. It means that the partial transfer charge (spin) occurs between these two parts of molecule. The number of electron transferring during the first oxidation is smaller than one – it confirms our suggestion. Two parallel reactions after the first oxidation are possible (Scheme 6): (1) chemical reaction in piperazine part (I), the electrochemical oxidation of nitrogen atom at aromatic part II (0.36 V) and electron transfer from catecholate, the third stage (0.94 V) transition to *o*-quinone and (2) intramolecular one-electron transfer leading to *o*-semiquinone and its oxidation.

The similar second wave (0.40 V) is observed in the case of complex **2**, where the same fact is insufficiently expressed and, as the consequence, the main trend is the intramolecular one-electron transfer between nitrogen atom and catecholate fragment.

The redox potentials of complex $Ph_3Sb[4,5\text{-}Piperaz\text{-}3,6\text{-}DBCat]$ (**4**) are close to those for compound **1**, but the products of chemical reactions after oxidation have the different nature. The 1,4-diazabicyclo[2,2,2]octane is quasi-reversibly oxidized at 0.48 V under experimental conditions, and it is known that the relatively stable radical cation is formed during electrochemical oxidation process [18]. The electrolysis (0.58 V, Pt-working electrode) of the solution of $Ph_3Sb[4,5\text{-}Piperaz\text{-}3,6\text{-}DBCat]$ (**4**), during 2 h leads to the appearance of new waves in cathode region (Supplementary Fig. S5, curve 3). One of them is quasi-reversible reduction *o*-quinone obtained as the product of disproportionation reaction. This fact confirms the possibility of intramolecular one-electron transfer between nitrogen atom and pentamerous metallocycle via aromatic linker (Scheme 7).

The electrochemical irreversibility of the redox process in case intramolecular electron transfer is also observed in ferrocene derivatives with phenolate fragments [19].

The analysis of redox potentials (Table 3) points out that the values of $E^3_{1/2}$ for complexes **1**,**2**,**4** are close to the second oxidation potential of $Ph_3Sb(4\text{-}MeO\text{-}3,6\text{-}DBCat)$ corresponding the transition "*o*-semiquinone – *o*-quinone". If nitrogen donor group has effect on the second oxidation process (0.36–0.40 V) but the third oxidation stage, which is actually identical to the second transition for $Ph_3Sb(3,6\text{-}DBCat)$, is nearly insensitive to the nature of substituent in fourth position of Cat ligand. The value of the second oxidation potential for **3** is accurately close to values of the first oxidation potentials for **1** and **4**. It means that in this case the same nitrogen-addressed oxidation occurs.

However, we cannot rule out completely the possibility of another situation where first oxidation stage is the oxidation of catecholate to o-semiquinone with the following charge redistribution between SQ and nitrogen-containing group at fourth position of chelating ligand. In this case, the low reversibility of process points out to the subsequent reactions of nitrogen-centered cations leading to dealkylation, cycle opening, etc.

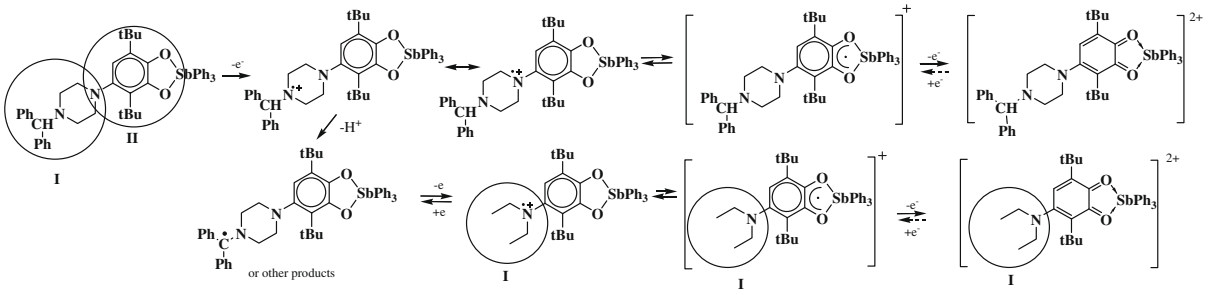

**Scheme 6.**

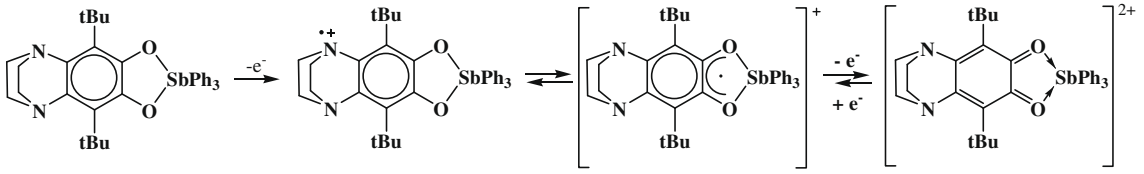

**Scheme 7.**

*2.5.2. Air exposure conditions*

The exposition of complexes solutions to air leads to the change in electrochemical behaviour.

Catecholato triphenylantimony(V) complexes which are able to the reversible dioxygen binding (for example, $Ph_3Sb$(4-MeO-3,6-DBCat) [7]) demonstrate the stability of one-electron oxidized semiquinonato forms; the peak oxidation potential is 0.34 V (vs. $Fc^+$/Fc couple) (see Table 3). The interaction of $Ph_3Sb$(4-MeO-3,6-DBCat) with dioxygen results in a decrease of the current magnitude of oxidation process Cat/SQ because, in fact, the dioxygen-bound form (spiroendoperoxide) has no catecholate form of ligand. The heating of dichloromethane solutions up to boiling point as well as the inert gas (e.g. argon) passing through the solution restores the initial picture of CV. These results confirm the reversible character of dioxygen binding by 4-methoxy derivative $Ph_3Sb$(4-MeO-3,6-DBCat). We have examined complexes **1**–**4** in the same manner.

Like 4-methoxy-catecholate complex $Ph_3Sb$(4-MeO-3,6-DBCat), the exposition of catecholates **1**–**4** solutions to air results in decrease of oxidation current magnitude. Fig. 5 shows CV of complex **3** in different conditions: without air and on air with the use of cycle "oxidation-regeneration". For complexes **2**–**4**, the proportional decrease of oxidation current magnitudes for both redox-processes (the first and second oxidations) takes place pointing out the electronic interaction of two redox-active parts of molecules. Such simultaneous decrease of first and second oxidation waves confirms the proposed scheme of electron density transfer between two redox-centers (amine and catecholate) despite of their remoteness. If there was no the interaction between these redox-active centers, one would expect that the first oxidation peak would be unchanged or just shifted slightly. (It means that the oxidation of catecholate fragment would not influence the redox-properties of piperazine cycle, but it is not the case). For catecholate **1**, the peak current drops twice only for the second but not the first oxidation wave which is practically not changed. It means that the interaction of two redox-centers in complex **1** is less pronounced than in complexes **2**–**4**.

Under the dioxygen-binding, new oxidation peaks (1.10 V for **1a**, 0.6 V for **2a**, 0.73 V for **3a** and 1.02 V for **4a**) can be observed which disappears with the solution heating. The heating leads to restoring of initial catecholates **1**–**4** peaks and their approaching of oxidation current magnitudes to the initial values.

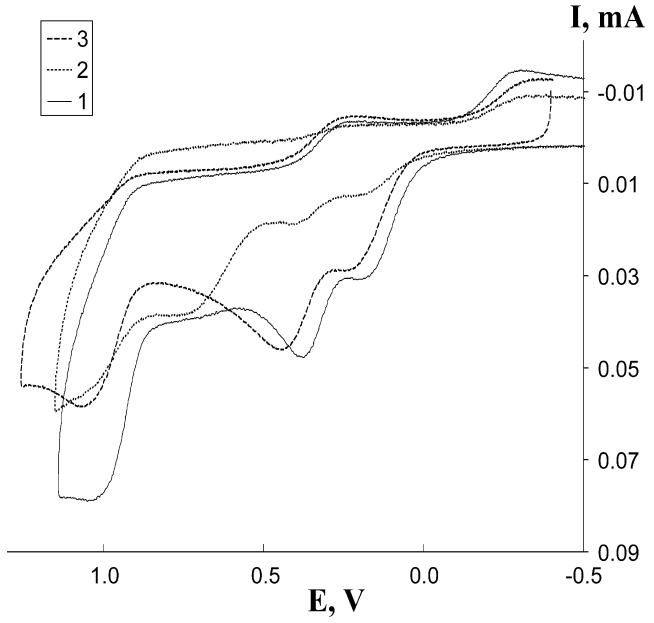


**Fig. 5.** Cyclic voltammogram of initial complex **3** ($3 \times 10^{-3}$ M) (1); after exposure of oxygen (2); after heating solution (3) in $CH_2Cl_2$ solution (0.10 M $Bu_4NClO_4$), platinum working electrode at scan rates of 200 mV $s^{-1}$. Potentials are referenced in volts vs. $Fc^+$/Fc.

So, in all cases the dioxygen binding takes place, electrochemical studies confirm NMR spectroscopic data and show that dioxygen binding is partially reversible, the heating of complexes' solutions after exposition to air restore starting complexes. It is obvious from electrochemical data, that the electronic interaction between the amine-containing group in fourth position of catecholato center and Cat fragment affect the electrochemical behaviour of complexes as well as their dioxygen-binding activity.

## 3. Conclusions

We have synthesized and characterized in details a series of triphenylantimony(V) catecholates containing weak donor morpholine and piperazine groups in fourth (or 4,5-) position of 3,6-

di-*tert*-butyl-catecholate ligand. Like catecholates with strong donor substituents, new complexes also react with molecular oxygen to form spiroendoperoxides that was confirmed by $^1$H NMR spectroscopy and cyclic voltammometry. However, the insertion of weak donor groups to Cat ligand in $Ph_3SbCat$ (instead of strong methoxy groups as in [7]) leads to the less efficient oxygen binding, the conversion of catecholates to spiroendoperoxides is 25–37% contrary to ~85% for triphenylantimony(V) catecholates with strong donor groups. Also, the $^1$H NMR spectroscopic studies allow to propose the formation of geometrical isomers of spiroendoperoxides with different relative positions of N-donor group and peroxo-fragment – the more preferred *para*- and the less preferred *meta*-isomers. The cyclic voltammometry studies on complexes corroborate results of NMR spectroscopic investigation: a dioxygen binding is partially reversible. Cyclic voltammometry shows that complexes undergo a series of one-electron oxidations. The electronic interaction between the amine-containing group in fourth position of catecholato center and Cat fragment affect the electrochemical behaviour of complexes as well as their dioxygen-binding activity.

## 4. Experimental

### 4.1. General considerations

Solvents were purified by standard methods [20]. Syntheses of complexes **1**–**5** were carried out in vacuum. $^1$H NMR spectra were recorded on Bruker AVANCE DPX-200 spectrometer, using the $CDCl_3$ solvent and the internal standard tetramethylsilane. IR spectra were recorded on Specord M-80. X-ray structure analysis was carried out on "Smart Apex" diffractometer (Bruker AXS).

Electrochemical studies were carried out using IPC-Pro potentiostate in three-electrode mode. The stationary glassy carbon ($d$ = 2 mm) disk was used as working electrode, the auxiliary electrode was a platinum-flag electrode. The reference electrode was a Ag/AgCl/KCl (sat.) with watertight diaphragm and ferrocene was added as internal standard ($E_{Fc+/Fc}$ = 0.42 V vs. Ag/AgCl). All measurements were carried out under argon. The samples were dissolved in the pre-deaerated solvent. The rate scan was 200 mV s$^{-1}$. The supporting electrolyte 0.1 M $Bu_4NClO_4$ (99%, "Acros") was undergone twice recrystallization from aqueous EtOH and then it was dried in vacuum (48 h) under 50 °C.

### 4.2. Preparation of complexes

Triphenylantimony (0.35 g, 1 mmol) was dissolved in dry toluene (20 ml) and a sample of corresponding *o*-benzoquinone $Q^1$–$Q^4$ (1 mmol) dissolved in 20 ml of toluene was added dropwise to the triphenylantimony solution over a period of 10 min. After the addition was complete, the reaction mixture became yellow or yellow–orange. Removal of solvent under vacuum yielded a solid material. Recrystallization of this crude material from appropriate solvent (see below) yielded microcrystalline product. In all cases yield was more 90%.

#### 4.2.1. (3,6-Di-tert-butyl-4-morpholine-4-yl-catecholato)triphenylantimony(V) (**1**)

The pure sample of complex **1** was isolated by the recrystallization from pentane as the pale yellow powder. Yield is 91%. m.p. 149 °C, at $t$ > 180 °C decomposes.

Anal. Calc. for $C_{36}H_{42}NO_3Sb$: C, 65.66; H, 6.43; Sb, 18.49. Found: C, 66.02; H, 6.39; Sb, 18.20%. IR (nujol, cm$^{-1}$): 1492 w, 1478 w, 1435 m, 1390 m, 1355 w, 1290 w, 1257 m, 1095 s, 1065 m, 1036 w, 1024 w, 998 w, 979 m, 937 m, 921 w, 850 w, 826 w, 813 s, 781 w, 731 s, 694 s, 623 m, 581 w, 543 w, 519 w, 497 w, 456 m. $^1$H NMR ($CDCl_3$), $\delta$, ppm: 1.41 and 1.60 (both s, both 9H, 2 *t*Bu), 2.64 and 2.70 (m, both 1H, $-CH_2CH_2-$ groups), 2.93-3.06 (t (1:2:1) d, 2H, $-CH_2CH_2-$ groups), 3.66–3.90 (m, 4H, $-CH_2CH_2-$ groups), 6.63 (s, 1H, $C_6H_1$), 7.39–7.52 (m, 9H, $SbPh_3$), 7.70–7.82 (m, 6H, $SbPh_3$). $^{13}$C NMR ($CDCl_3$, $\delta$, ppm): 29.56 and 32.49 ($CH_3$ of *t*Bu), 34.46 and 36.53 (*C* of *t*Bu), 54.86 ($O(CH_2–CH_2)_2N–$), 67.37 ($O(CH_2–CH_2)_2N–$), 111.65 (*C*H of Ar), 128.45 (Ar), 129.08 ($SbPh_3$), 131.02 ($SbPh_3$), 131.79 (Ar), 135.03 ($SbPh_3$), 138.02 ($SbPh_3$), 142.40 (*C*–N of Ar), 143.10 (*C*–O of Ar), 145.67 (*C*–O of Ar). $^{13}$C{$^1$H} NMR ($CDCl_3$, $\delta$, ppm): 29.56, 32.49, 54.86, 67.37, 111.65, 129.08, 131.02, 135.03.

#### 4.2.2. (3,6-Di-tert-butyl-4-(4-phenylpiperazine-1-yl)-catecholato)triphenylantimony(V) (**2**)

The pure **2** isolated from hexane is brightly yellow powder. Yield is 93%. m.p. 171–172 °C (decomp.).

Anal. Calc. for $C_{42}H_{47}N_2O_2Sb$: C, 68.76; H, 6.46; Sb, 16.60. Found: C, 68.49; H, 6.42; Sb, 16.82%. IR (nujol, cm$^{-1}$): 1599 m, 1577 m, 1534 w, 1501 m, 1443 s, 1412 w, 1376 s, 1354 m, 1337 m, 1296 m, 1268 w, 1259 w, 1232 m, 1202 w, 1191 w, 1180 w, 1147 m, 1107 m, 1082 w, 1072 m, 1063 m, 1033 w, 1025 w, 1006 w, 997 w, 978 m, 941 m, 929 m, 906 m, 870 w, 858 w, 850 w, 840 w, 851 m, 781 m, 753 m, 728 s, 690 s, 664 m, 631 m, 617 m, 597 m, 568 w, 545 w, 520 m, 500 m, 466 m, 455 m, 444 s. $^1$H NMR ($CDCl_3$), $\delta$, ppm: 1.42 and 1.61 (both s, both 9H, 2 *t*Bu), 2.91-3.11 and 3.51-3.59 (m, 8H, 2 $-CH_2CH_2-$), 6.70 (s, 1H, $C_6H_1$), 6.86 (t, $^4J_{(H,H)}$ = 7.3 Hz, 1 *para*-H, Ph), 6.98 (t, $^4J_{(H,H)}$ = 8.0 Hz, 2 *ortho*-H, Ph), 7.27 (t, $^4J_{(H,H)}$ = 7.5 Hz, 2 *meta*-H, Ph), 7.40–7.54 (m, 9H, $SbPh_3$), 7.70-7.84 (m, 6H, $SbPh_3$). $^{13}$C NMR ($CDCl_3$, $\delta$, ppm): 29.61 and 32.60 ($CH_3$ of *t*Bu), 34.49 and 36.59 (*C* of *t*Bu), 49.68 and 54.63 ($-N(CH_2-CH_2)_2N–$), 111.44 (*C*H of Ar), 116.18 (o-*C*H of Ph), 119.55 (p-*C*H of Ph), 128.42 (Ar), 129.04 (m-*C*H of Ph), 129.09 ($SbPh_3$), 131.02 ($SbPh_3$), 131.77 (Ar), 135.04 ($SbPh_3$), 138.06 ($SbPh_3$), 142.49 (*C*–N of Ar), 143.14 (*C*–O of Ar), 145.71 (*C*–O of Ar), 151.90 (i-*C* of Ph). $^{13}$C{$^1$H} NMR ($CDCl_3$, $\delta$, ppm): 29.61, 32.60, 49.68, 54.63, 111.44, 116.18, 119.55, 129.04, 129.09, 131.02, 135.04.

#### 4.2.3. (3,6-Di-tert-butyl-4-(4-diphenylmethylpiperazine-1-yl)-catecholato)triphenylantimony(V) (**3**)

The bright-yellow powder was isolated from the mixture hexane-toluene (1:1). Yield is 89%. decomp. >150 °C.

Anal. Calc. for $C_{49}H_{53}N_2O_2Sb$: C, 71.45; H, 6.49; Sb, 14.78. Found: C, 71.78; H, 6.43; Sb, 15.01%. IR (nujol, cm$^{-1}$): 1599 w, 1588 m, 1537 w, 1461 s, 1434 s, 1392 s, 1378 s, 1355 m, 1331 m, 1300 m, 1281 m, 1240 m, 1228 m, 1194 m, 1181 w, 1160 w, 1134 m, 1101 w, 1086 m, 1073 m, 1061 m, 1031 m, 1016 w, 1004 m, 981 m, 963 w, 933 m, 924 m, 866 w, 854 m, 838 w, 824 w, 813 m, 783 m, 745 s, 731 s, 710 s, 692 s, 665 w, 655 m, 625 m, 611 w, 597 w, 569 m, 542 w, 531 m, 514 s, 499 s, 466 s, 454 s, 443 s, 416 w. $^1$H NMR ($CDCl_3$), $\delta$, ppm: 1.43 and 1.56 (both s, both 9H, 2 *t*Bu), 2.17–2.21 and 2.69–2.98 (both m, 8H, 2 $-CH_2CH_2-$), 4.21 (s, 1H, CH), 6.70 (s, 1H, $C_6H_1$), 7.15–7.50 (m, 6H, 2Ph), 7.39–7.50 (m, 9H, $SbPh_3$ and 4H, 2Ph), 7.73-7.77 (m, 6H, $SbPh_3$). $^{13}$C NMR ($CDCl_3$, $\delta$, ppm): 29.67 and 32.54 ($CH_3$ of *t*Bu), 34.48 and 36.51 (*C* of *t*Bu), 52.74 and 54.79 ($-N(CH_2-CH_2)_2N–$), 77.09 ($Ph_2CH–$), 111.61 (*C*H of Ar), 126.79 (p-*C*H of Ph), 127.96 and 128.44 (o- and m-*C*H of Ph), 128.45 (Ar), 129.06 ($SbPh_3$), 130.98 ($SbPh_3$), 131.62 (Ar), 135.04 ($SbPh_3$), 138.09 ($SbPh_3$), 142.80 (*C*-N of Ar), 142.94 (*C*–O of Ar), 143.28 (i-*C* of Ph), 145.62 (*C*–O of Ar). $^{13}$C{$^1$H} NMR ($CDCl_3$, $\delta$, ppm): 29.67, 32.54, 52.74, 54.79, 77.09, 111.61, 126.79, 127.96, 128.44, 129.06, 130.98, 135.04.

*4.2.4. (3,6-Di-tert-butyl-4,5-(N,N'-diethylenediamine)-catecholato)triphenylantimony(V) (**4**)*

Complex **4** was isolated from pentane as described for **1**. Yield is 94%. m.p. 210–212°C (decomp.).

Anal. Calc. for $C_{36}H_{41}N_2O_2Sb$: C, 65.96; H, 6.30; Sb, 18.58. Found: C, 66.02; H, 6.39; Sb, 18.20%. IR (nujol, $cm^{-1}$): 1568 s, 1532 s, 1478 s, 1433 s, 1347 s, 1333 s, 1302 m, 1295 m, 1273 m, 1260 s, 1235 s, 1225 s, 1190 m, 1158 w, 1070 s, 1053 s, 1042 s, 1022 m, 995 s, 988 s, 936 s, 922 m, 900 w, 870 m, 854 s, 825 m, 774 s, 731 s, 693 s, 660 m, 631 m, 616 w, 597 w, 563 m, 531 m, 522 m, 471 m, 446 s. $^1$H NMR ($CDCl_3$), $\delta$, ppm: 1.60 (s, 18H, 2 *t*Bu), 2.54–2.75 (m, 4H, $-CH_2CH_2-$), 2.86–3.07 (m, 4H, $-CH_2CH_2-$), 7.36–7.61 (m, 9H, $SbPh_3$), 7.67–7.81 (m, 6H, $SbPh_3$). $^{13}$C NMR ($CDCl_3$, $\delta$, ppm): 32.33 (*C*H$_3$ of *t*Bu), 35.46 (*C* of *t*Bu), 50.12 ($-N(CH_2-CH_2)_2N-$), 126.44 (Ar), 129.01 ($SbPh_3$), 130.93 ($SbPh_3$), 135.09 ($SbPh_3$), 138.09 ($SbPh_3$), 141.20 (*C*–N of Ar), 143.62 (*C*-O of Ar). $^{13}C\{^1H\}$ NMR ($CDCl_3$, $\delta$, ppm): 32.33, 50.12, 129.01, 130.93, 135.09. The prolonged crystallization of yellow product from methanol gave X-ray quality crystals of **4** as the methanol solvate (**4**·$CH_3OH$).

*4.2.5. 4,4′-(Piperazine-1,4-diyl)-bis(3,6-di-tert-butyl-catecholato)triphenylantimony(V) (**5**)*

This complex was prepared by the same method as for **1**–**4** from $Ph_3Sb$ (0.138 g, 0.39 mmol) and 4,4′-(piperazine-1,4-diyl)bis(3,6-di-*tert*-butyl-*o*-benzoquinone) (0.102 g, 0.195 mmol). Pure sample of **5** was recrystallized from a hexane–toluene mixture (1:1) as bright-yellow microcrystalline powder.

Anal. Calc. for $C_{68}H_{76}N_2O_4Sb_2$: C, 66.46; H, 6.23; Sb, 19.82. Found: C, 66.28; H, 6.09; Sb, 20.00. IR (nujol, $cm^{-1}$): 1603 w, 1588 w, 1578 w, 1535 w, 1494 w, 1477 s, 1434 s, 1390 s, 1321 m, 1288 m, 1244 s, 1191 m, 1158 w, 1131 m, 1097 s, 1076 m, 1061 m, 1027 m, 1001 s, 998 s, 985 s, 935 s, 849 m, 814 m, 787 m, 730 s, 693 s, 665 m, 625 m, 576 w, 531 w, 503 m, 469 s, 457 s, 449 s, 428 m, 419 m, 407 s. $^1$H NMR ($CDCl_3$), $\delta$, ppm: 1.44 and 1.66 (both s, both 18H, 4 *t*Bu), 2.73–2.76 and 3.03–3.07 (both m, 8H, 2 $-CH_2CH_2-$), 6.72 (s, 2H, $2C_6H_1$), 7.44–7.47 (m, 18H, 2 $SbPh_3$), 7.75–7.79 (m, 12H, 2 $SbPh_3$). $^{13}$C NMR ($CDCl_3$, $\delta$, ppm): 29.63 and 32.69 (*C*H$_3$ of *t*Bu), 34.74 and 36.61 (*C* of *t*Bu), 55.05 ($-N(CH_2-CH_2)_2N-$), 111.63 (*C*H of Ar), 128.49 (Ar), 129.05 ($SbPh_3$), 130.96 ($SbPh_3$), 131.56 (Ar), 135.09 ($SbPh_3$), 138.20 ($SbPh_3$), 142.81 (*C*–N of Ar), 143.51 (*C*–O of Ar), 145.59 (*C*–O of Ar). $^{13}C\{^1H\}$ NMR ($CDCl_3$, $\delta$, ppm): 29.63, 32.69, 55.05, 111.63, 129.05, 130.96, 135.09.

### 4.3. X-ray diffraction studies

Suitable crystals for X-ray diffraction were prepared by prolonged crystallization of **4** from methanol solution as methanol solvate **4**·$CH_3OH$.

Intensity data were collected on a Smart Apex diffractometer with graphite monochromated Mo Kα radiation ($\lambda$ = 0.71073 Å) in the $\varphi$–$\omega$ scan mode ($\omega$ = 0.3°, 10 s on each frame). Absorption corrections were made by SADABS program [21]. The structures were solved by direct methods and refined on $F^2$ by full matrix least squares using SHELXTL [22]. All non-hydrogen atoms were refined anisotropically. The hydrogen atoms were found from Fourier syntheses of electron density and refined isotropically. Crystallographic data and structure refinement details are given in Table 2. The CCDC-733150 (**4**·$CH_3OH$) contains the supplementary crystallographic data for this paper. These data can be obtained free of charge via www.ccdc.cam.ac.uk/conts/retrieving.html (or from the Cambridge Crystallographic Data Centre, 12 Union Road, Cambridge CB21EZ, UK; fax: (+44) 1223-336-033; or deposit@ccdc.cam.ac.uk).

## Supplementary material

Supplementary material includes the Supplementary Figs. S1-S5 – $^1$H NMR of **5** on air and cyclic voltammograms of complexes **1**-**4**. Crystallographic data have been deposited with the Cambridge Crystallographic Data Centre, CCDC No. 249948 for **4**·$CH_3OH$. Copies of this data may be obtained free of charge from The Director, CCDC, 12 Union Road, Cambridge CB2 1EZ, UK (Fax: +44-1223-336033; email: deposit@ccdc.cam.ac.uk).

## Acknowledgements

We are grateful to the Russian Foundation for Basic Research (Grants 10-03-00921 and 10-03-00850), Russian President Grants (Grants NSh-7065.2010.3, NSh-1396.2008.3, MK-3364.2010.3, MK-1286.2009.3), Russian Science Support Foundation (A.I. Poddel'sky) for financial support of this work.

## Appendix A. Supplementary data

Supplementary data associated with this article can be found, in the online version, at doi:10.1016/j.jorganchem.2010.01.029.

## References

[1] (a) See for example: M.D. Ward (Ed.), Comprehensive Coordination Chemistry II: Applications of Coordination Chemistry, vol. 9, Elsevier, Amsterdam, 2005, pp. 305–360;
(b) J.P. Finet, Ligand Coupling Reactions with Heteroatomic Compounds, Pergamon, New York, 1998;
(c) A.V. Gushchin, E.V. Grunova, D.V. Moiseev, O.S. Morozov, A.S. Shavyrin, V.A. Dodonov, Russ. Chem. Bull. 52 (2003) 1376–1379;
(d) A. Saito, M. Umakoshi, N. Yagyu, Yu. Hanzawa, Org. Lett. 10 (2008) 1783–1785.
[2] (a) J. Reglinski, in: N.C. Norman (Ed.), The Chemistry of Arsenic, Antimony and Bismuth, Blackie, London, 1998 (Chapter 8, Environmental and medicinal chemistry of arsenic, antimony and bismuth);
(b) U. Wormser, I. Nir, in: S. Patai (Ed.), Chemistry of Organic Arsenic, Antimony and Bismuth Compounds, Wiley, New York, 1994, pp. 715–723 (Chapter 18, Pharmacology and toxicology of organic bismuth, arsenic and antimony compounds);
(c) R. Ge, H. Sun, Acc. Chem. Res. 40 (2007) 267–274;
(d) I.I. Ozturk, S.K. Hadjikakou, N. Hadjiliadis, N. Kourkoumelis, M. Kubicki, M. Baril, I.S. Butler, J. Balzarini, Inorg. Chem. 46 (2007) 8652–8661;
(e) P. Sharma, D. Perez, A. Cabrera, N. Rosas, J.L. Arias, Acta Pharmacol. Sin. 29 (2009) 881–890;
(f) H.P.S. Chauhan, U.P. Singh, Appl. Organomet. Chem. 21 (2007) 880–889;
(g) K. Mahajan, M. Swami, S.C. Joshi, R.V. Singh, Appl. Organomet. Chem. 22 (2008) 359–368;
(h) S.K. Hadjikakou, I.I. Ozturk, M.N. Xanthopoulou, P.C. Zachariadis, S. Zartilas, S. Karkabounas, N. Hadjiliadis, J. Inorg. Biochem. 102 (5–6) (2008) 1007–1015.
[3] (a) R.M. Buchanan, C.G. Pierpont, J. Am. Chem. Soc. 102 (1980) 4951–4957;
(b) G.A. Abakumov, V.I. Nevodchikov, V.K. Cherkasov, Dokl. Akad. Nauk. SSSR 278 (1984) 641–645;
(c) G.A. Abakumov, G.A. Razuvaev, V.I. Nevodchikov, V.K. Cherkasov, J. Organomet. Chem. 341 (1988) 485–494;
(d) D. Ruiz-Molina, J. Veciana, K. Wurst, D.N. Hendrickson, C. Rovira, Inorg. Chem. 39 (2000) 617–619;
(e) M.W. Lynch, D.N. Hendrickson, B.J. Fitzgerald, C.G. Pierpont, J. Am. Chem. Soc. 103 (1981) 3961–3963;
(f) Osamu Sato, Jun Tao, Angew. Chem., Int. Ed. 46 (2007) 2152–2187.
[4] (a) G.A. Abakumov, V.I. Nevodchikov, Dokl. Akad. Nauk. SSSR 266 (1982) 1407–1410;
(b) C.W. Lange, M. Foldeaki, V.I. Nevodchikov, V.K. Cherkasov, G.A. Abakumov, C.G. Pierpont, J. Am. Chem. Soc. 114 (1992) 4220–4222;
(c) O.-S. Jung, C.G. Pierpont, J. Am. Chem. Soc. 116 (1994) 2229–2230.
[5] M.I. Kabachnik, N.N. Bubnov, A.I. Prokof'ev, S.P. Solodovnikov, Science Rev. XXIV (1981) 197. and references therein.
[6] G.A. Abakumov, A.I. Poddel'sky, E.V. Grunova, V.K. Cherkasov, G.K. Fukin, Yu.A. Kurskii, L.G. Abakumova, Angew. Chem., Int. Ed. 44 (2005) 2767–2771.
[7] (a) G.A. Abakumov, V.K. Cherkasov, E.V. Grunova, A.I. Poddel'sky, L.G. Abakumova, Yu.A. Kurskii, G.K. Fukin, E.V. Baranov, Dokl. Chem. 405 (2005) 222–225;
(b) V.K. Cherkasov, G.A. Abakumov, E.V. Grunova, A.I. Poddel'sky, G.K. Fukin, E.V. Baranov, Yu.A. Kurskii, L.G. Abakumova, Chem. Eur. J. 12 (2006) 3916–3927.
[8] (a) V.K. Cherkasov, E.V. Grunova, A.I. Poddel'sky, G.K. Fukin, Yu.A. Kurskii, L.G. Abakumova, G.A. Abakumov, J. Organomet. Chem. 690 (2005) 1273–1281;
(b) A.I. Poddel'sky, I.V. Smolyaninov, Yu.A. Kurskii, N.T. Berberova, V.K.

Cherkasov, G.A. Abakumov, Russ. Chem. Bull. 58 (3) (2009) 520–525 (in Russian).
[9] (a) M. Hall, D.B. Sowerby, J. Am. Chem. Soc. 102 (2) (1980) 628–632;
(b) Z. Tian, D.G. Tuck, J. Chem. Soc., Dalton Trans. (1993) 1381–1385;
(c) G.K. Fukin, L.N. Zakharov, G.A. Domrachev, A.U. Fedorov, S.N. Zaburdyaeva, V.A. Dodonov, Russ. Chem. Bull. 9 (1999) 1744–1753;
(d) R.R. Holmes, R.O. Day, V. Chandrasekhar, J.M. Holmes, Inorg. Chem. 26 (1987) 157–163;
(e) M.N. Gibbons, M.J. Begley, A.J. Blake, D.B. Sowerby, J. Chem. Soc., Dalton Trans. (1997) 2419–2425.
[10] G.A. Abakumov, V.K. Cherkasov, T.N. Kocherova, N.O. Druzhkov, Yu.A. Kurskii, M.P. Bubnov, G.K. Fukin, L.G. Abakumova, Rus. Chem. Bull. 56 (2007) 1849–1856.
[11] (a) L.G. Abakumova, VI Fechem Conference on Organometallic Chemistry, Riga 1985, Book of Abstracts, 1985, 185.;
(b) P.A. Wicklund, L.S. Beckmann, D.G. Brown, Inorg. Chem. 15 (1976) 1996–1997;
(c) D.R. Lide (Ed.), Handbook of Chemistry and Physics, 84th ed., CRC Press, 2003–2004, pp. 9-86–9-90.
[12] (a) C.G. Pierpont, Coord. Chem. Rev. 219–221 (2001) 415–433;
(b) A.I. Poddel'sky, V.K. Cherkasov, G.A. Abakumov, Coord. Chem. Rev. 253 (2009) 291–324.
[13] P. Zanello, M. Corsini, Coord. Chem. Rev. 250 (2006) 2000–2022.
[14] H. Lund, O. Hammerich, Organic Electrochemistry, 4th ed., Marcel Dekker Inc., New York, 2001.
[15] V.G. Koshechko, S.A. Shpil'nyi, V.D. Pokhodenko, Theor. Exp. Chem. 32 (1) (1996) 27–29.
[16] Sun Hanwen, Xing Tao, Lian Kaoqi, Liang Shuxuan, Chem. J. Intern. 8 (8) (2006) 53.
[17] (a) C.K. Mann, K.K. Barns, Electrochemical Reactions in Nonaqueous Systems, Marcel Dekker Inc., New York, 1970;
(b) M. Warowna-Grzeskiewicz, J. Chodkowski, Z. Fijalek, Acta. Pol. Pharm. 52 (1995) 187.
[18] T.M. McKinney, D.H. Genske, J. Am. Chem. Soc. 87 (1965) 3013.
[19] E.A. Hillard, P. Pigeon, A. Vessieres, C. Amatore, G. Jaouen, Dalton Trans. (2007) 5073–5081.
[20] D.D. Perrin, W. L.F Armarego, D.R. Perrin, Purification of Laboratory Chemicals, Pergamon, Oxford, 1980.
[21] G.M. Sheldrick, SADABS v.2.01, Bruker/Siemens Area Detector Absorption Correction Program, Bruker AXS, Madison, WI, USA, 1998.
[22] G.M. Sheldrick, SHELXTL v. 6.12, Structure Determination Software Suite, Bruker AXS, Madison, WI, USA, 2000.